Environmental Science Nano

Mechanistic study of oil adsorption onto PVP-coated magnetic nanoparticles: An integrated experimental and molecular dynamics study to inform remediation

Journal:	*Environmental Science: Nano*
Manuscript ID	EN-ART-09-2020-000907.R1
Article Type:	Paper

ARTICLE

Mechanistic study of oil adsorption onto PVP-coated magnetic nanoparticles: An integrated experimental and molecular dynamics study to inform remediation

Linkel K. Boateng[a], Seyyedali Mirshahghassemi[b], Haibin Wu[c], Joseph R.V. Flora[a], Vicki H. Grassian[c,*], Jamie R. Lead[b,*]

Received 00th January 20xx,
Accepted 00th January 20xx

DOI: 10.1039/x0xx00000x

Abstract

Nanotechnology has recently sparked considerable interest as a cleanup technique for oil remediation. Although several studies have been reported in this area the mechanisms of the surface processes involved in the adsorption of oil onto nanoparticles (NPs) are still not clearly elucidated. Here, we combine molecular dynamics (MD) simulations and experimental data using ATR-FTIR spectroscopy to show that polyvinylpyrrolidone (PVP) polymer interacts physically with magnetite cluster via van der Waals with an average binding strength of –9.2 kcal mol^{-1}. The results indicate that the adsorption of crude oil onto PVP-coated magnetic NPs is thermodynamically favorable with an adsorption free energy of –3.6 kcal mol^{-1}. However, crude oil adsorption reduces in the presence of fulvic acid (FA), which is attributed to the ability of FA to partially displace PVP in seawater and form a new coating layer on the magnetite surface. Our work highlights the implications of molecular interactions and environmental conditions on the adsorption of crude oil onto NPs, which is critical for the effective design of nano-based oil remediation strategies.

Environmental significance

The limitations in traditional clean up techniques for oil remediation have inspired the application of nanotechnology for oil removal. However, the mechanisms of the surface processes involved in the adsorption of oil onto nanoparticles are poorly understood. Understanding the mechanisms governing crude oil interactions with nanoparticles is critical for developing effective nano-based oil remediation techniques. Here, we adopt an integrated experimental and computational approach to study the adsorption of crude oil onto nanoparticles under relevant environmental conditions. The results indicate that fulvic acid influences crude oil adsorption onto nanoparticles via an interplay of co-adsorption and intermolecular interactions. Our study provides important mechanistic insight for developing nano-based oil remediations and understanding the different surface processes involved in crude oil adsorption.

Introduction

The application of nanoparticles (NPs) for oil removal from oil spills and wastes has been widely studied (1, 2) due to the limitations in traditional clean up techniques.(3-5) Other related studies have also focused on the development of advanced oil sorbents capable of extracting oil from water.(6-8) As previously discussed, many synthesis methods are multistep, which makes scale up difficult and expensive compared to our facile and cheap hydrothermal approach for synthesizing polyvinylpyrrolidone (PVP)-coated magnetite NPs.(9) Moreover, the majority of studies involving NPs have been conducted under simple laboratory conditions and the behavior and performance of NPs under real conditions have rarely been investigated.(10, 11) In order to assess the practical application of NPs for oil remediation, studies under relevant environmental conditions must be explored to evaluate the effectiveness of NP-based remediation techniques. In addition, the mechanisms of the surface processes involved in the adsorption of oil onto magnetic NPs must be elucidated under such environmentally relevant conditions. Atomistic simulations can provide unique insight of the molecular interactions between NPs and crude oil to elucidate adsorption mechanisms, which is critical for the effective design of nano-based remediation strategies. Molecular dynamics (MD) simulations have been extensively used to evaluate intermolecular binding and adsorption mechanisms between different NPs and various adsorbates.(12-15) MD simulations can provide microscopic-level description of NP-adsorbent interactions to rationalize experimental findings. For instance, Bürger et al. adopted MD simulations to establish that the adsorption of amino acids onto Fe-terminated magnetite-(111)-surface was energetically favorable and was predominately due to electrostatic interactions.(14)

In the present study, we use Attenuated Total Reflection Fourier Transform Infrared (ATR-FTIR) spectroscopy and MD simulations to investigate the surface processes involved in using NPs for the successful removal of oil from the aqueous phase.(16-19) A combination of experimental studies and computational modeling is useful for probing mechanisms at different scales to improve data quality and depth and provide confidence in data. This approach is expected to provide insight on the nature and strength of PVP interaction with Fe_3O_4 cluster, as well as crude oil adsorption onto magnetite NPs under realistic environmental conditions.

ATR-FTIR spectroscopy was employed to probe a PVP-coated Fe_3O_4 NP film to study the interaction between PVP and Fe_3O_4 NPs, crude oil and PVP-coated NPs and investigate the stability of the

[a] Department of Civil and Environmental Engineering, University of South Carolina, Columbia, SC, 29208, United States
[b] Center for Environmental Nanoscience and Risk (CENR), Department of Environmental Health Sciences, Arnold School of Public Health, University of South Carolina, Columbia, South Carolina 29208, United States
E-mail: jlead@mailbox.sc.edu; Fax: +1 (803) 777 3391; Tel: +1 (803) 777 0091
[c] Department of Chemistry & Biochemistry, University of California San Diego, La Jolla, 92093, United States

Electronic Supplementary Information (ESI) available: ATR-FTIR spectra data on adsorption experiments under flowing conditions.
See DOI: 10.1039/x0xx00000x

coatings on Fe_3O_4 NPs in seawater under different environmental conditions. The binding of a PVP monomer onto a magnetite cluster in seawater was simulated to probe the nature and strength of PVP-magnetite interactions. To effectively simulate the occurrence of possible chemical reactions between potential reactive points on the PVP and $(Fe_3O_4)_3$ molecules, MD simulations coupled with umbrella sampling(20) were conducted to quantity the binding of the carbonyl oxygen in the PVP onto Fe^{2+} and Fe^{3+} atoms in the $(Fe_3O_4)_3$ cluster.(21) A mechanistic insight on crude oil interaction with PVP-coated NPs was obtained by conducting simulations to quantify the binding strength of crude oil onto PVP-coated NP in the presence of salt and natural organic matter (NOM) (representative of environmental conditions, where oil remediation would occur).

Methodology

Experimental Studies

The preparation of synthetic seawater follows the EPA recommended seawater composition: Milli–Q water, sodium chloride (NaCl, Fisher Chemicals, ACS grade), sodium sulfate (Na_2SO_4, Fisher Chemicals, ACS grade), potassium chloride (KCl, Fisher Chemicals, ACS grade), potassium bromide (KBr, Aldrich, 99%), sodium tetraborate decahydrate ($Na_2B_4O_7{\cdot}10H_2O$, 99%+), magnesium chloride hexahydrate ($MgCl_2{\cdot}6H_2O$, Fisher Chemicals, ACS grade), calcium chloride dehydrate ($CaCl_2{\cdot}2H_2O$, MP Biomedicals, 99%), strontium chloride hexahydrate ($SrCl_2{\cdot}6H_2O$, Avantor, ACS grade), and sodium bicarbonate ($NaHCO_3$, Fisher Chemicals, ACS grade). All solutions containing organic compounds were prepared using synthetic seawater. In this study, crude oil, a representative of Deepwater Horizon oil spill (reference MC 252 surrogate oil, sample ID: A0068H, AECOM Environment) was used. Also, Suwannee River fulvic acid (International Humic Substances Society) was used to represent natural organic macromolecules present in ocean water.

PVP-coated magnetic NPs were synthesized using a modified hydrothermal method previously reported.(9) In summary, 0.18 mmol of PVP (Mw 10 kDa, Sigma-Aldrich) was added to 6.25 ml ultrapure water while the solution was stirred at 80 ± 5 ºC. 1 mmol of $FeCl_2.4H_2O$ (98%, Alfa Aesar) and 4 mmol of $FeCl_3{\bullet}6H_2O$ (>98%, BDH) were added to the solution and stirred while the temperature was kept constant. Next, 0.12 mmol PVP was dissolved and finally 6.25 mL ammonium hydroxide (28-30%, BDH) was added to the solution dropwise at room temperature while the solution was stirred. The suspension was mixed for 25 min at 90± 5 ºC and the precipitate was washed once with deionized water and separated by magnetic decantation to remove impurities. The NPs were re-dispersed in water again via sonication and stored for later use. The details of NPs characterization including atomic force microscopy (AFM), thermogravimetric analysis (TGA), Fourier transform infrared spectrometry (FTIR), dynamic light scattering (DLS), and X-ray powder diffraction (XRD) data have been published previously.(9, 22)

ATR–FTIR spectra were recorded using a horizontal ATR cell with an AMTIR element (Pike Technologies Inc.). The cell was placed inside a Nicolet iS10 FTIR spectrometer equipped with an MCT–A detector. The NP film was made by drying 1 mL of the as-synthesized Fe_3O_4 NP solution on an AMTIR crystal in a dry air environment overnight. Different solutions were then added to the cell with the NP film. A glass cover was placed over the flow cell followed by spectral collection. All spectra were collected by acquiring 1000 scans at an instrument resolution of 4 cm^{-1} in the spectral range extending from 750 to 4000 cm^{-1}. For solution phase spectra, 1 mL seawater was added on the AMTIR crystal with a NP film. A glass cover was placed over the flow cell and a background spectrum was immediately collected. Next, the seawater was carefully removed after collecting a background, and 1 mL of FA (10 ppm, 20 ppm or 50 ppm) was added onto the same film. The spectra were collected after 2-hour adsorption. Crude oil mainly consists of saturated and unsaturated hydrocarbons and is immiscible in polar solvents such as water. In order to promote the adsorption of crude oil on Fe_3O_4 NPs, a crude oil suspension was rotated with dispersed NPs. For the spectrum of a dry PVP-Fe_3O_4 NP film after crude oil adsorption, 10 mL PVP coated NP solution was centrifuged for 10 min at 10,000 rpm to separate the NPs from the solution. Then, 10 mL of crude oil suspension (1.7 g/L) was added to the NPs after removing the supernatant. The solutions were sonicated for 30 min and placed onto a Cole-Parmer rotator for 48 hrs. After the adsorption, the NPs were re-dispersed in 10 mL Milli-Q water. 1mL of the NP solution was added onto an AMTIR crystal dry overnight in a dry air environment. In the case of FA–PVP–Fe3O4 NPs, the NPs were exposed to FA solution prior to crude oil adsorption. For the spectrum of a dry FA-PVP-Fe_3O_4 NP film after crude oil adsorption, the NPs were separated from 10 mL of stock solution by centrifugation and exposed to 10 mL of 50 ppm FA for 24 hrs. prior to crude oil adsorption. After adsorption process of FA, the NPs were re–dispersed in crude oil solution for 48 hrs. Afterwards, the NPs were centrifuged and dispersed in 10 mL Milli–Q water. 1 mL suspension of NPs in water was placed onto an AMTIR crystal drying overnight. The spectrum of dry film was collected to study crude oil adsorption.

Molecular Simulations

The molecular model of the NP was constructed using the Atomsk modeling tool.(23) Because we are interested in the NP-PVP surface interactions, a cut-out of a 10 nm diameter NP was used in the molecular dynamics simulations to reduce computational time in the simulations. A PVP polymer model was constructed to match the experimental properties by sequencing 90 PVP units to form a PVP polymer chain. Initially, 3 PVP polymer chains were randomly located in a large periodic box and equilibrated to form a PVP polymer with the desired density. In this study, humic acid (HA) is chosen as a representative NOM molecule to investigate its influence on oil adsorption. The HA structure is based on the Temple-Northeastern-Birmingham (TNB) molecular model which consists of carboxyl, phenolic and amine functional groups.(24) The TNB HA has properties similar to Suwanee river NOM which was used in the experiments. All simulations were performed with the LAMMPS(25) computational package and results visualized using visual molecular dynamics.(26) For the simulations involving possible chemical reactions, a magnetite cluster with three Fe_3O_4 units with a PVP monomer was solvated in explicit water and simulated using the reaxFF force field(27) developed for amine iron oxide system.(28) The reaxFF force field has been widely used to simulate bond formation and breakage. For all other simulations, the consistent valence force field (CVFF)(29) was used to describe the interactions between the PVP polymer while the NP interactions were described using the clayFF forcefield.(30) The CVFF has been shown to be consistent with the clayFF force field. A PVP-NP complex was solvated in TIP3P water. Sodium, calcium, potassium and chloride ions were added to create a representative hard water and seawater systems. In our experiments, PVP is generally only slightly charged and the NPs are nearly uncharged at neutral pH, therefore, a near neutral pH is maintained in the simulations. The solvated systems were initially minimized for 10,000 steps and equilibrated at a constant volume for 1 ns. The system was further equilibrated at a constant pressure of 1bar using Berendsen's barostat with the PVP atoms harmonically restrained with a force constant of 10 kcal mol^{-1}

Å^{-1}. All atoms of the NP were fixed during the simulations. A 10 ns production simulation was conducted under the NVT ensemble without restraints on the PVP atoms at constant temperature and volume. The Langevin thermostat was used to maintain a temperature of 300 K in the simulations. The long-range electrostatic interactions were calculated using the particle-particle mesh solver(31) and the cutoff distance for the short-range Lennard-Jones interactions was set to 10 Å. All bonds involving hydrogen atoms were restrained to their equilibrium value using the SHAKE algorithm. Periodic boundary conditions were applied in all directions. The velocity Verlet scheme was adopted to propagate the equation of motions with a time step of 2 fs. In the umbrella sampling simulations, a harmonic restraint of 20 kcal mol^{-1} Å^{-1} was applied to restrain the center-to-center distances of the PVP and the respective adsorbates. The intermolecular distances were varied from the minimum separation to distances where interactions were negligible in 0.1 nm increments. Umbrella sampling windows were simulated for 1 ns saving data at 10 ps interval for analysis.

Results and discussion

The result of the ATR-FTIR spectroscopy study is shown in Fig. 1a, together with the MD simulation configuration (Fig. 1b) and the potential of mean force (PMF) describing the strength of PVP interaction with $(Fe_3O_4)_3$ as a function of interatomic distance (Fig. 1 c). As indicated in the spectra, the PVP coating (black line in Fig. 1a) shows a broad absorption from 1200 – 1700 cm^{-1} associated with different vibrational motions. For example, the peak at 1658 cm^{-1} is assigned to the stretching mode of the C=O in PVP and multiple peaks from 1200 – 1600 cm^{-1} (labeled in the light grey area) represent bending modes of CH or CH_2 groups.(32, 33)

It can be observed that, the bending modes of CH or CH_2H in PVP molecules(9, 34) in the range 1250 – 1700 cm^{-1} diminishes after exposure to seawater indicating the partial desorption of PVP in seawater. The amount of PVP left on the NP surface following exposure to seawater is estimated to be ~10 % based on the integrated area of the peaks in the spectral area extending from 1250 to 1350 cm^{-1}. This frequency of carbonyl stretching in PVP on the NP surface is similar to the reported values for pure PVP, indicating that carbonyl functional groups may interact with metal cations on NP surface through electrostatic attraction or hydrogen bonds with hydroxyl groups on NP oxide surfaces.(35) The other broad absorption ca. 3400 cm^{-1} is the stretching motion of O–H or adsorbed water on NPs, and the bending mode of water adsorbed on NP surfaces near 1638 cm^{-1} is overlapped with PVP carbonyl absorption. It can be seen that absorption at 1658 cm^{-1} shown in the PVP coated Fe_3O_4 film changes to ~1638 cm^{-1} after exposure to seawater which is associated with the bending mode of adsorbed water or hydroxyl group on NP surfaces (red curve in Fig. 1a), suggesting partial desorption of PVP from the NP surface. Thus, PVP is not strongly bound onto NP and partially desorbs from the NP surface when in contact with seawater.

This observation is consistent with the results of the simulations which suggest a physical interaction between PVP and the $(Fe_3O_4)_3$ cluster. As shown in the PMF above, PVP-O interacts favorably with Fe^{2+} and Fe^{3+} atoms at a minimum interatomic separation of 0.15 nm with corresponding binding energies of –9.5 and –8.9 kcal mol^{-1}, respectively. A negative PMF value indicates attraction while a positive PMF represents repulsion relative to the free energy at a separation of 1.0 nm. As the interatomic distance increases, the PMF becomes flat indicating negligible interaction between Fe and PVP-O atoms. Although the computed PVP-$(Fe_3O_4)_3$ interactions are significant, experimental bond dissociation energies for Fe and PVP-O are on the order of 97.3 kcal mol^{-1}(36), which is significantly

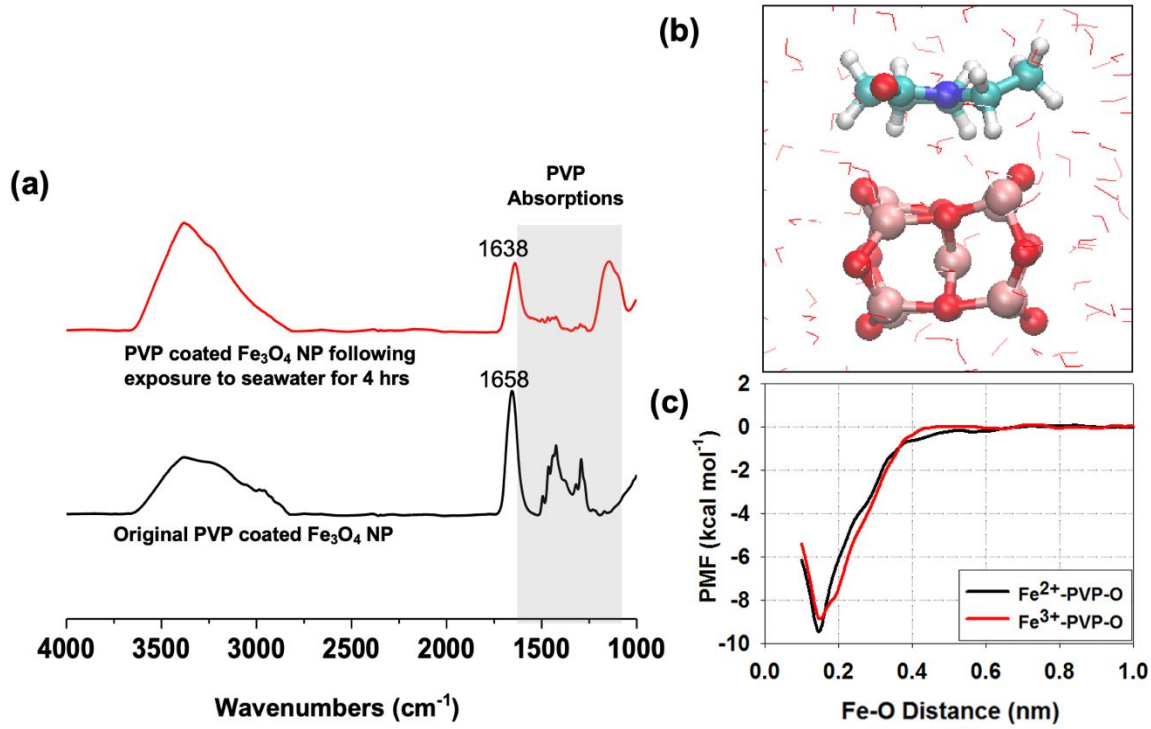

Fig. 1. (a) PVP Coating Stability. Baseline corrected ATR-FTIR spectra of a thin film of PVP-coated Fe_3O_4 NPs before (black) and after (red) exposure to seawater for 4 hrs. (b) PVP-Fe_3O_4 complex in water; PVP and $(Fe_3O_4)_3$ are shown in CPK model and water molecules shown as lines (c) PMF describing the free energy of binding of PVP-O onto Fe atoms.

stronger than the resulting binding energies from the above PMFs. The weak binding of PVP onto $(Fe_3O_4)_3$ cluster suggests that interactions between $(Fe_3O_4)_3$ and PVP atoms are mainly physical,

mostly due to van der Waals interactions.(12) Thus, both experimental and simulation results indicate a weak binding of PVP onto $(Fe_3O_4)_3$ cluster in seawater suggesting that PVP is physically sorbed onto $(Fe_3O_4)_3$ in solution through multiple points of attachment.

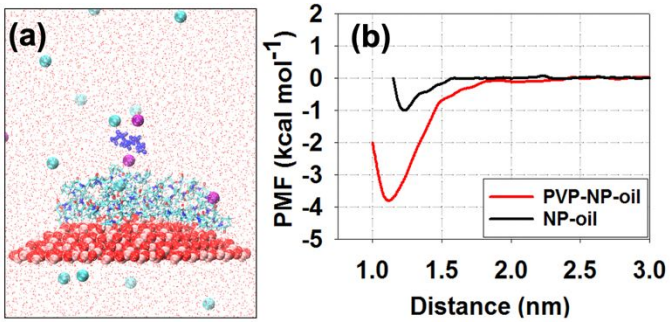

Fig. 2. (a) PVP-coated NP with oil in water; NP is shown in VDW model, PVP is shown in licorice model, oil is shown in blue licorice model, Na^+, K^+ and Cl^- ions are shown as spheres and water molecules shown as red dots (b) PMF describing the binding free energy of crude oil adsorption onto pristine NP and PVP-coated NP.

Recent experimental studies have shown that PVP-coated NPs can be used to achieve nearly 100 % oil removal from water.(9, 22, 37) Here, we used nonane as a representative hydrocarbon to simulate crude oil adsorption onto PVP-coated NPs. Although crude oil consists of chemically complex compounds, simulating nonane can provide insight on the nature of molecular interactions involved in adsorption to obtain preliminary data to study more complex mixtures. An initial molecular configuration of the system was built by randomly locating nonane molecule on the surface of a PVP-coated NP as shown in Fig. 2a. We first simulated nonane interaction with both uncoated and PVP-coated NPs to evaluate binding mechanisms and binding contributions from the different adsorbents. The resulting PMF is shown in Fig. 2b as a function of the separation distance between PVP and oil. Due to the hydrophilic nature of the surface of the pristine NP, oil interaction with the uncoated NP is less favorable with a binding energy of only –1.0 kcal mol^{-1}. However, in the case of the of PVP-coated NP, there is an increased oil interaction, thus, the presence of the PVP coating significantly increased oil binding from –1.0 to –3.6 kcal mol^{-1}. The increased adsorption is attributed to the fact that oil sorption is likely driven by hydrophobic effect, with hydrophobic moieties of the PVP coating allowing preferential sorption of hydrocarbons from the oil-water mixture onto the PVP-coated NPs.(38) It should be noted that the binding of oil onto the PVP-coated NPs is primarily driven by weak, physical Van der Waals interactions, with multiple points of contact.

We also performed further experiments and simulations to investigate the effect of NOM on the adsorption of oil onto PVP–coated NPs. In our experiments, Suwannee River FA (SRFA) is chosen as a representative model of NOM with reasonable abundance in aqueous environments.(39) FA has a complex macromolecular structure with conjugated aromatic rings and polar functional groups (e.g. phenol, amide and carboxylic acid groups).(40) The interaction of FA and PVP–Fe_3O_4 NPs was investigated via ATR–FTIR by adding 1 mL synthetic seawater solutions containing various concentrations of FA at pH 7.9 on a PVP–Fe_3O_4 NP film after 2 hours adsorption. Fig. 3a shows ATR–FTIR spectra of adsorbed FA on these NP films. As indicated in the figure, the two negative peaks observed in the spectra at 1290 and 1652 cm^{-1} is due to the partial desorption of PVP. The peaks at 1390 and 1570 cm^{-1} correspond to FA carboxylate symmetric and asymmetric stretching, respectively. Humic acid (HA) and FA have been reported to strongly bind onto metal oxide surface regardless of pre-coated molecules.(40, 41) These two types of NOM are able to chemically bind to metal oxide surfaces, via their multifunctional groups e.g. carboxylate and phenol.(40-42) A previous study shows FA strongly adsorbs on metal oxide surfaces, resulting in an irreversible adsorption onto metal oxide surface.(43) Our ATR-FTIR results confirm that FA is able to adsorb onto the PVP-coated Fe_3O_4 NPs and the intensity does not show notable decrease after flowing seawater onto the FA adsorbed Fe_3O_4 NP film for 30 min (Fig. S1 in supporting information). The simulation results indicate a favorable interaction between PVP coating and the simulated HA molecule in seawater (Fig. 3b). As indicated in Fig. 3c, HA strongly

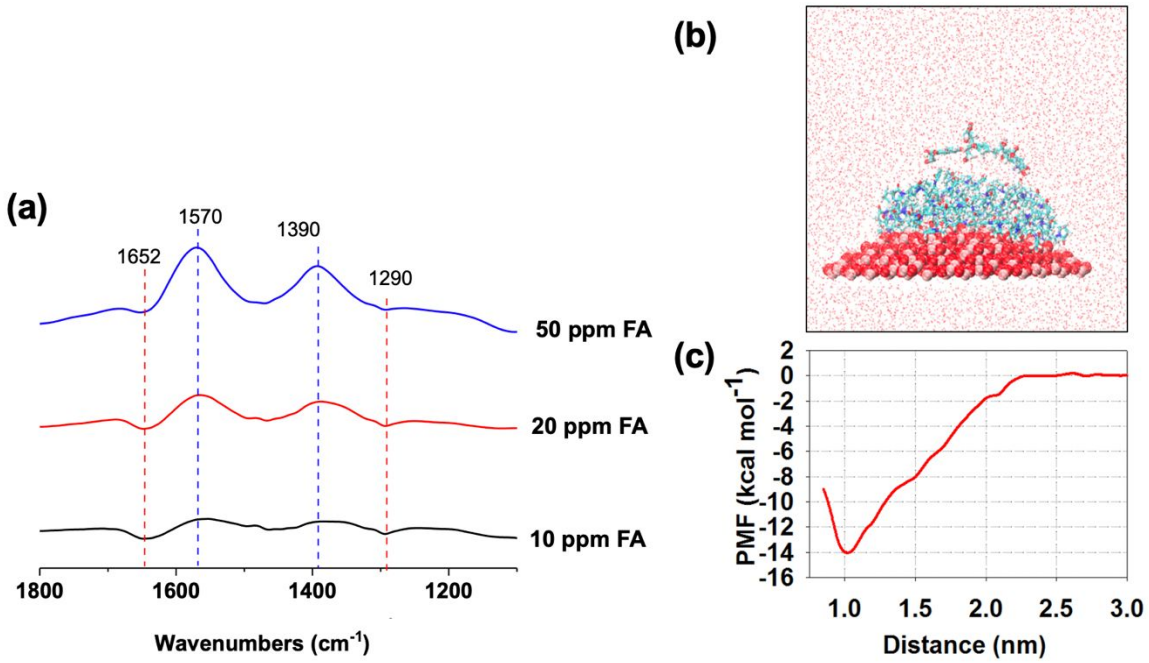

Fig. 3. (a) ATR-FTIR spectra of various concentrations of fulvic acid in seawater on PVP- Fe_3O_4 NP films. The spectra show that absorptions associated with FA carboxylate groups (at 1390 and 1570 cm^{-1}) increase with increasing FA concentrations labeled with blue dash lines. Simultaneously, PVP desorbs from the surface as shown by the negative features at 1290 and 1652 cm^{-1} labeled with red dash lines. (b) PVP-coated NP-NOM complex in water (c) PMF describing the binding free energy of NOM adsorption onto PVP-coated NP.

binds onto the PVP-coated NP surface with a free binding energy of –14.0 kcal mol^{-1}. Although the nature of this interaction is physical, with increased HA concentration, HA adsorption onto PVP-coated NP can become irreversible and be classified as a pseudo-chemical interaction.

The favorable interaction between HA and the PVP-coated NP indicates a strong affinity for the adsorption of HA onto Fe_3O_4 NPs as observed in the experiments.

The splitting of symmetric and asymmetric stretching of a carboxylate suggests the binding coordination of carboxylate onto the NP surface. The magnitude of splitting in this case around 180 cm^{-1} in the spectra normally indicates a carboxylate is binding to a surface through a bridging mode in which a carboxylate group binds with two adjacent metal ions on the surface.(44, 45) We observed that negative desorption peaks of PVP and positive adsorption peaks border appear in the spectra when FA solution is placed on the PVP-Fe_3O_4 NP film. Thus, it is possible that FA adsorbs onto NPs simultaneously with the partial desorption of PVP from the iron oxide surface in seawater and that this behavior is dependent on solution conditions.

Our recent study indicates that FA can act as a competitive phase for either PVP or oil and reduce oil interaction with NPs.(22) To further probe the effect of this mechanism on oil adsorption, HA interaction with oil, PVP monomer and PVP-coated NP were simulated to quantify the binding strength for the different cases. As presented in Fig. 4b, the interaction of HA with oil (snapshot shown in Fig. 4a) is slightly stronger (–5.1 kcal mol^{-1}) than the interaction with PVP (–3.5 kcal mol^{-1}) in the aqueous phase. The stronger binding between HA and oil suggest that the formation of HA-oil complexes is likely, which can lead to increased aqueous solubility of oil. The increased oil solubility will likely drive oil away from the surface of the PVP-coated NP to reduce oil removal from the aqueous phase.

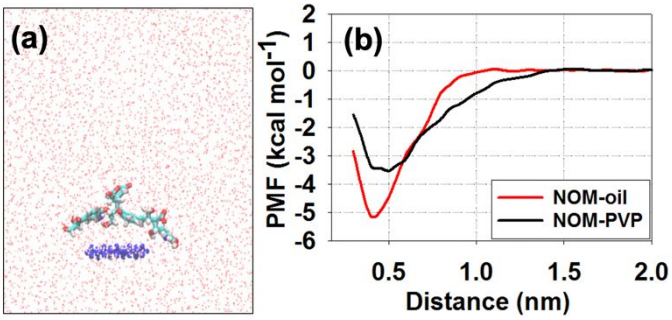

Fig. 4. (a) NOM-oil complex in water; NOM is shown in licorice model, oil is shown in blue licorice model and TIP3P water molecules shown as points (b) PMF describing the binding free energy of NOM interaction with crude oil and PVP.

The dry films of crude oil adsorbed NPs were investigated via ATR-FTIR spectra shown in Fig. 5. The three peaks observed in the 2800 to 3000 cm^{-1} range are associated with C–H stretching vibrations, while the two peaks at 1381 and 1464 cm^{-1} are associated with CH_2 and CH_3 deformation modes.(46) As observed in Fig. 5, a comparison of the spectrum for the crude oil suspension in seawater (indicated in blue) with the other two spectra following adsorption indicates an increase in absorbance but no changes in frequency. This suggests that crude oil interacts with NPs mainly via hydrophobic interactions and the adsorption behavior is influenced by the presence of FA. It is evident that coatings on NPs favors adsorption of crude oil. However, the spectrum following adsorption of crude oil on FA–PVP–Fe_3O_4 NPs shows slightly lower absorbance than the one on PVP–Fe_3O_4 NPs, indicating that the presence of FA may reduce the adsorption of oil in agreement with previous results.(9, 22) The favorable interaction between FA and PVP–Fe_3O_4 NPs makes FA a strong competitive adsorbate to potentially block oil adsorption onto NPs. It is possible that FA is more favorable to competitively adsorb onto the active sites than oil molecules inhibiting oil adsorption onto

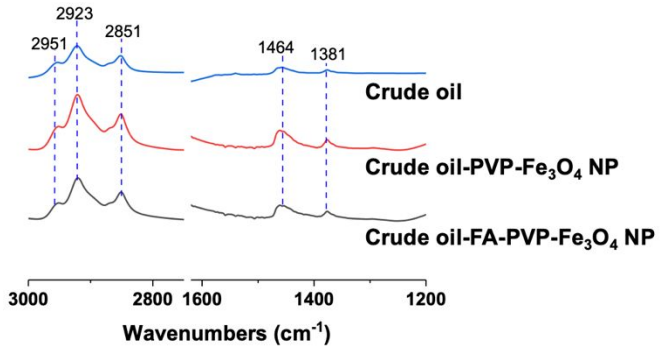

Fig. 5. Crude oil adsorption on PVP-Fe_3O_4 NPs in absence and presence of FA. ATR–FTIR spectra in the region extending from 1200 to 1610 and 2775 to 3000 cm^{-1} of ~1.7 g/L crude oil solution (blue), a dry NP film after adsorption of crude oil on PVP–Fe_3O_4 NPs (red), and a dry NP film after adsorption of crude oil on FA –PVP–Fe_3O_4 NPs. These spectra show that FA does not impact crude oil adsorption on the NP surface.

the NPs. Our recent work has shown that natural filtered waters behave differently compared to environmentally relevant waters with extracted NOM of apparently identical composition. This is attributed to the complexity of unperturbed NOM compared to that of extracted NOM(47).

The different surface processes involved in the adsorption of oil onto PVP-coated Fe_3O_4 NPs are presented in the schematic shown in Fig. 6. As illustrated, the PVP coating on Fe_3O_4 NP is not stable in seawater and consequently, desorbs partially from the surface of the Fe_3O_4 NP. Thus, PVP partially desorbs from the surface in the presence of salt and FA, forming a new layer. In the presence of FA, FA molecules are able to partially displace PVP and form a new coating layer on the NP surface. It is worth noting that some PVP molecules may not be directly displaced by FA but through intermolecular interaction with FA due to steric effect on some sites. This results in co-adsorption and intermolecular interaction, which enables crude oil to be readily adsorbed onto the new surface through intermolecular interaction with FA. Moreover, as observed in our previous study(9), the crude oil covered NPs would further aggregate by forming micron sized globules in the presence of ions, which can result in increased crude oil adsorption. These mechanisms are currently being investigated via molecular dynamics simulations. Future studies will also consider the use of a more complex crude oil model and a slightly charged PVP-coated NP surface to capture the different types of interactions involved in crude oil adsorption.

Conclusion

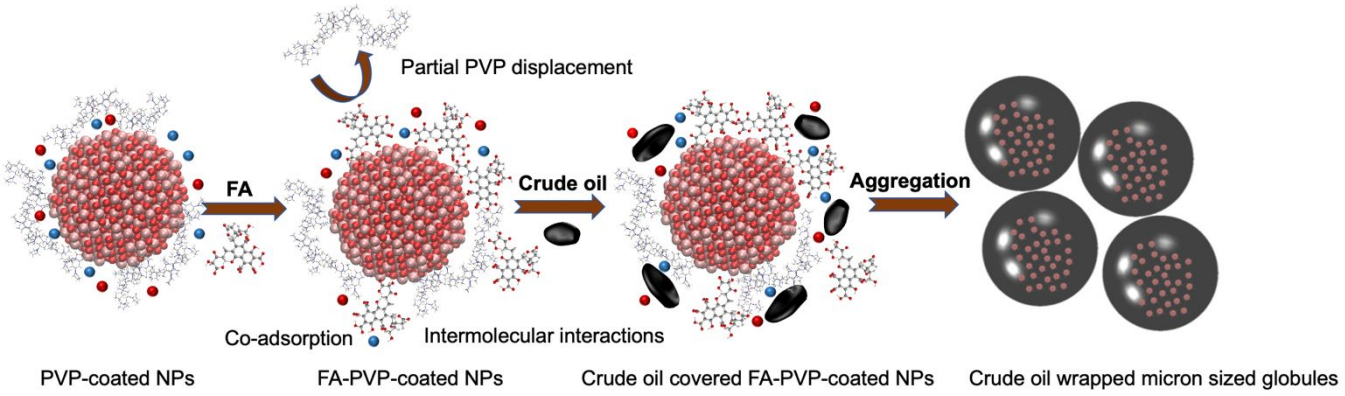

Fig. 6. Schematic of surface processes for PVP coated Fe_3O_4 NPs in the presence of FA and crude oil. The processes occur in an ion-rich environment representing by blue and dark red dots. Initial PVP is unstable in seawater and can be readily displaced by FA to form new FA-PVP coatings. The adsorbed crude oil on new coating surface aggregate into micron size globules of oil and NPs.[19]

The results of an integrated experimental and MD simulations study have shown favorable adsorption of crude oil onto PVP-coated magnetic NPs in the presence of NOM. The results indicate that PVP is physically sorbed onto the surface of $(Fe_3O_4)_3$ cluster through multiple points of attachment via van der Waals interactions. In the presence of FA, the PVP coating on the magnetic NPs is partially displaced, resulting in the formation of a new coating layer, which consequently reduces oil adsorption. The reduced oil adsorption is attributed to reduced non-polar hydrophobic interactions between oil molecules and the magnetic NPs surface. Thus, the presence of FA influences crude oil adsorption onto NPs via an interplay of co-adsorption and intermolecular interactions.

Conflicts of interest

There are no conflicts to declare.

Acknowledgements

The authors wish to thank UofSC Research Cyberinfrastructure for the computing time used in this research.

References

1. Su C. Environmental implications and applications of engineered nanoscale magnetite and its hybrid nanocomposites: A review of recent literature. J Hazard Mater. 2016.

2. Lei W, Portehault D, Liu D, Qin S, Chen Y. Porous boron nitride nanosheets for effective water cleaning. Nat Commun. 2013;4:1777.

3. National Commission on the BP Deepwater Horizon Oil Spill and Offshore Drilling, Deep Water: the Gulf Oil Disaster and the Future of Offshore Drilling. Washington, D.C.: UNT Digital Library; 2014.

4. The Federal Interagency Solutions Group, Oil Budget Calculator Science and Engineering Team, Oil Budget Calculator, Deepwater Horizon-Technical Document. http://www.noaanews.noaa.gov/stories2010/PDFs/OilBudgetCalc_Full_HQ-Print_111110.pdf . 2010.

5. Fritz DE. I*n Situ* Burning of Spilled Oil in Freshwater Inland Regions of the United States. Spill Sci Technol Bull. 2003;8:331-5.

6. Nandwana V, Ribet SM, Reis RD, Kuang Y, More Y, Dravid VP. OHM Sponge: A Versatile, Efficient, and Ecofriendly Environmental Remediation Platform. I*nd Eng Chem Res*. 2020;59(23):10945–54.

7. Barry E, Libera JA, Mane AU, Avila JR, DeVitis D, Dyke KV, et al. Mitigating oil spills in the water column. Environ Sci: Water Res Technol. 2018;4:40-7.

8. Xiong S, Zhong Z, Wang Y. Direct silanization of polyurethane foams for efficient selective absorption of oil from water. *AIChE J*. 2017;*63*:2232–40.

9. Mirshahghassemi S, Lead JR. Oil Recovery from Water under Environmentally Relevant Conditions Using Magnetic Nanoparticles. Environ Sci Technol. 2015;49(19):11729-36.

10.Jiang G, Hu R, Wang X, Xi X, Wang R, Wei Z, et al. Preparation of superhydrophobic and superoleophilic polypropylene fibers with application in oil/water separation. J Text Inst. 2013;104(8):790-7.

11.Song S, Yang H, Zhou C, Cheng J, Jiang Z, Lu Z, et al. Underwater superoleophobic mesh based on BiVO4 nanoparticles with sunlight-driven self-cleaning property for oil/water separation. Chem Eng. 2017;320:342-51.

12.Grasso G, Deriu MA, Prat M, Rimondini L, Verne E, Follenzi A, et al. Cell Penetrating Peptide Adsorption on Magnetite and Silica Surfaces: A Computational Investigation. J Phys Chem B. 2015;119:8239-46.

13.Park OK, Tiwary CS, Yang Y, Bhowmick S, Vinod S, Zhang Q, et al. Magnetic field controlled graphene oxide-based origami with enhanced surface area and mechanical properties. Nanoscale. 2017;9:6991-7.
14.Bürger A, Magdans U, Gies H. Adsorption of amino acids on the magnetite-(111)-surface: a force field study. J Mol Model. 2013;19:851–7.
15.Yue J, Jiang X, Yu A. Molecular Dynamics Study on Au/Fe_3O_4 Nanocomposites and Their Surface Function toward Amino Acids. . J Phys Chem B. 2011;115:11693–9.
16.Peijnenburg W, Baalousha M, Chen JW, Chaudry Q, Von der kammer F, Kuhlbusch TAJ, et al. A Review of the Properties and Processes Determining the Fate of Engineered Nanomaterials in the Aquatic Environment. Crit Rev Environ Sci Technol. 2015;45:2084-134.
17.Loosli F, Le Coustumer P, Stoll S. Effect of electrolyte valency, alginate concentration and pH on engineered TiO2 nanoparticle stability in aqueous solution. Sci Total Environ. 2015;535:28-34.
18.Afshinnia K, Gibson I, Merrifield R, Baalousha M. The concentration-dependent aggregation of Ag NPs induced by cystine. 2016;557-558:395-403.
19.Al-Hamadani YAJ, Chu KH, Son A, Heo J, Her N, Jang M, et al. Stabilization and dispersion of carbon nanomaterials in aqueous solutions: A review. 2015;156 (Part 2):861-74.
20.Torrie GM, Valleau JP. Nonphysical sampling distributions in Monte Carlo free-energy estimation: Umbrella sampling. Journal of Computational Physics. 1977;23(2):187-99.
21.Im JK, Boateng LK, Flora JRV, Her N, Zoh KD, Son A, et al. Enhanced ultrasonic degradation of acetaminophen and naproxen in the presence of powdered activated carbon and biochar adsorbents. Sep Purif Technol. 2014;123:96-105.
22.Mirshahghassemi S, Cai B, Lead JR. Evaluation of polymer-coated magnetic nanoparticles for oil separation under environmentally relevant conditions: effect of ionic strength and natural organic macromolecules. Environ Sci Nano. 2016;3(4):780-7.
23.Hirel P. Atomsk: A tool for manipulating and converting atomic data files. Comput Phys Commun. 2015;197:212-9.
24.Sein LT, Varnum JM, Jansen SA. Conformational Modeling of a New Building Block of Humic Acid: Approaches to the Lowest Energy Conformer. Environ Sci Technol. 1999;33(4):546-52.
25.Plimpton S. Fast Parallel Algorithms for Short-Range Molecular Dynamics. J Comp Phys. 1995;117:1-19.
26.Humphrey W, Dalke A, Schulten K. VMD: visual molecular dynamics. J Mol Graph Model. 1996;14(1):33-8.
27.van Duin ACT, Dasgupta S, Lorant F, Goddard WA. ReaxFF: A Reactive Force Field for Hydrocarbons. J Phys Chem A. 2001;105(41):9396-409.
28.Chia CL. Classical and ReaxFF Molecular Dynamics Simulations of Fuel Additives at the Solid-fluid Interface. Manchester: University of Manchester; 2018.
29.Kitson DH, Hagler AT. Theoretical studies of the structure and molecular dynamics of a peptide crystal. Biochemistry. 1988;27(14):5246-57.
30.Cygan RT, Liang J-J, Kalinichev AG. Molecular Models of Hydroxide, Oxyhydroxide, and Clay Phases and the Development of a General Force Field. J Phys Chem B. 2004;108(4):1255-66.
31.Hockney RW, Eastwood JW. Computer simulation using particles: Taylor & Francis Group; 1988. 564 p.
32.Song Y-J, Wang M, Zhang X-Y, Wu J-Y, Zhang T. Investigation on the role of the molecular weight of polyvinyl pyrrolidone in the shape control of high-yield silver nanospheres and nanowires. Nanoscale Res Lett. 2014;9(1):17.
33.Pandey G, Singh S, Hitkari G. Synthesis and characterization of polyvinyl pyrrolidone (PVP)-coated Fe_3O_4 nanoparticles by chemical co-precipitation method and removal of Congo red dye by adsorption process. Int Nano Lett. 2018;8(2):111-21.
34.Száraz I, Forsling W. PVP and azelaic acid adsorption on γ-alumina studied by FT-IR spectroscopy. Vib Spectrosc. 2002;29(1):15-20.
35.Borodko Y, Habas SE, Koebel M, Yang P, Frei H, Somorjai GA. Probing the interaction of poly(vinylpyrrolidone) with platinum nanocrystals by UV−Raman and FTIR. J Phys Chem B. 2006;110(46):23052-9.
36.Luo Y-R. Comprehensive handbook of chemical bond energies: CRC press; 2007.
37.Mirshahghassemi S, Ebner AD, Cai B, Lead JR. Application of high gradient magnetic separation for oil remediation using polymer-coated magnetic nanoparticles. Sep Purif Technol. 2017;179:328-34.
38.Song JE, Phenrat T, Marinakos S, Xiao Y, Liu J, Wiesner MR, et al. Hydrophobic Interactions Increase Attachment of Gum Arabic- and PVP-Coated Ag Nanoparticles to Hydrophobic Surfaces. Environ Sci Technol. 2011;45(14):5988-95.
39.Jackson tA. Humic matter in natural waters and sediments. Soil Sci. 1975;119(1):56-64.
40.Jayalath S, Larsen SC, Grassian VH. Surface adsorption of Nordic aquatic fulvic acid on amine-

functionalized and non-functionalized mesoporous silica nanoparticles. Environ Sci Nano. 2018;5(9):2162-71.
41.Wu H, Gonzalez-Pech NI, Grassian VH. Displacement reactions between environmentally and biologically relevant ligands on TiO_2 nanoparticles: insights into the aging of nanoparticles in the environment. Environ Sci Nano. 2019.
42.Jayalath S, Wu H, Larsen SC, Grassian VH. Surface Adsorption of Suwannee River Humic Acid on TiO_2 Nanoparticles: A Study of pH and Particle Size. Langmuir. 2018;34(9):3136-45.
43.Gu B, Schmitt J, Chen Z, Liang L, McCarthy JF. Adsorption and desorption of natural organic matter on iron oxide: mechanisms and models. Environ Sci Technol. 1994;28(1):38-46.
44.Dobson KD, McQuillan AJ. In situ infrared spectroscopic analysis of the adsorption of aliphatic carboxylic acids to TiO_2, ZrO_2, Al_2O_3, and Ta_2O_5 from aqueous solutions. Spectrochimica Acta Part A: Molecular and Biomolecular Spectroscopy. 1999;55(7):1395-405.
45.Dobson KD, McQuillan AJ. In situ infrared spectroscopic analysis of the adsorption of aromatic carboxylic acids to TiO_2, ZrO_2, Al_2O_3, and Ta_2O_5 from aqueous solutions. Spectrochimica Acta Part A: Molecular and Biomolecular Spectroscopy. 2000;56(3):557-65.
46.Petrov AA, Shtof IK. Investigation of structure of crude oil emulsion stabilizers by means of infrared spectroscopy. Chem Tech Fuels Oil. 1974;10(8):654-7.
47.Mirshahghassemi S, Cai B, Lead JR. A Comparison between the Oil Removal Capacity of Polymer-Coated Magnetic Nanoparticles in Natural and Synthetic Environmental Samples Environ Sci Technol. 2019;53:4426-32.

PVP coatings on magnetic NPs are partially displaced in the presence of fulvic acid, which reduces crude oil adsorption onto the magnetite.